

# Isomeric differentiation and quantification of $\alpha$ , $\beta$ -amino acid-containing tripeptides by the kinetic method: alkali metal-bound dimeric cluster ions

Lianming Wu<sup>a</sup>, Eduardo Cesar Meurer<sup>b</sup>, Brandy Young<sup>a</sup>, Pengxiang Yang<sup>a</sup>,  
Marcos N. Eberlin<sup>b</sup>, R. Graham Cooks<sup>a,\*</sup>

<sup>a</sup> Chemistry Department, Purdue University, West Lafayette, IN 47907, USA

<sup>b</sup> Institute of Chemistry, State University of Campinas, CP6154 Campinas, SP, 13083-970, Brazil

Received 2 July 2003; accepted 7 September 2003

Dedicated to Jean-Claude Tabet, the French typhoon, in appreciation of his science and especially his work in stereochemistry using mass spectrometry

## Abstract

The kinetic method is applied to differentiate and quantify mixtures of isomeric tripeptides by generating and mass-selecting alkali metal ion-bound dimeric clusters and examining their competitive dissociations in an ion trap mass spectrometer. This methodology readily distinguishes the pairs of isomers examined here:  $(\alpha\text{-A})\text{GG}/(\beta\text{-A})\text{GG}$ ,  $\text{G}(\alpha\text{-A})\text{G}/\text{G}(\beta\text{-A})\text{G}$ , and  $\text{GG}(\alpha\text{-A})/\text{GG}(\beta\text{-A})$ . The isomeric selectivity increases with decreasing size of the metal ion, viz. from Cs to Rb to K to Na to Li. When alanine is at the N-terminus, as in the case of  $(\alpha\text{-A})\text{GG}/(\beta\text{-A})\text{GG}$ , the isomeric selectivity can exceed  $10^3$ . The corresponding proton-bound dimers behave similarly to the Li clusters. Structural features that favor zwitterionic versus charge-solvated forms of the alkali metal-bound clusters are reflected in the  $b_n$  and  $y_n$  fragment ion abundances recorded by tandem mass spectrometry, and the propensities to form the charge-solvated or zwitterionic structures play a key role in promoting isomeric differentiation. The zwitterionic forms favor intramolecular interactions in the cluster and hence isomeric distinction. There is no discrimination in the formation of the alkali metal-bound dimers, so isomeric quantification is based entirely on dissociation kinetics. Previous kinetic method-based isomeric analyses have used the trimeric clusters and shown linear correlations between composition of the mixture of isomers and the logarithm of the branching ratio for competitive fragmentation. A similar relationship is found for the dimeric clusters examined here. As used here, the kinetic method provides a possible way for future quantitative analysis of mixtures of larger peptides such as those generated in combinatorial synthesis of peptides and peptide mimics.

© 2004 Elsevier B.V. All rights reserved.

**Keywords:** Kinetic method; Dissociation; Quantification; Isomeric tripeptides; Complexes; Central ion effects

## 1. Introduction

High and continuing interest in the characterization of peptides is driven by the increasing number of synthetic peptides developed for pharmaceutical applications [1]. Peptides control numerous biological processes, and, as such, represent a potential source of new drugs. Various non-natural biopolymers, including  $\beta$ -peptides and  $\gamma$ -peptides, represent new systems for testing the rules of protein folding and structural stabilization as well as providing an excellent

scaffold for the design of biomimetic structures with practical pharmaceutical applications [2].  $\beta$ -Peptides have particular appeal for extending our understanding of protein structure and stabilization into the realm of folded, non-natural polymers, because they represent the smallest step away from the  $\alpha$ -amino acids in “backbone space” [3]. Moreover,  $\beta$ -peptides adopt a variety of different helical conformations as the chirality is varied. Intriguingly, peptides comprised of  $\beta$ -amino acids share many properties with their  $\alpha$ -amino acid counterparts; but because  $\beta$ -amino acids are rarely found in nature,  $\beta$ -peptides are resistant enzymatic digestion, making them useful as pharmaceutical agents such as antibiotics. Consequently, research on the design of  $\beta$ -peptides for drug discovery is important in the development of “pep-

\* Corresponding author. Tel.: +1-765-494-5265; fax: +1-765-494-9421.  
E-mail address: [cooks@purdue.edu](mailto:cooks@purdue.edu) (R.G. Cooks).

tide mimetics”, with the potential to generate new drugs [4], especially those that might overcome the ineffectiveness of  $\alpha$ -peptides as drugs when administered orally.

The use of combinatorial libraries is expected to have a significant impact on drug discovery, including in the development and optimization of new leads. Methods that directly and easily analyze the purity of combinatorial mixtures, for example in the case of isomeric peptides that are not always easily distinguished, can provide information about the reliability of a synthetic protocol [5]. Therefore, this is a place for new, simple, fast and sensitive methods to determine isomeric purity [6]. We are working towards this rather large objective using the mass spectrometric kinetic method [7–10].

With the emergence of soft ionization techniques, such as electrospray ionization (ESI) [11] and matrix-assisted laser desorption ionization (MALDI) [12], the kinetic method has been extended to chiral analysis of amino acids [13], hydroxy acids [14], peptides [15], sugars [16], and several drugs such as antibiotics [17] and anti-viral nucleoside agent [18]. Recently, the method has also been extended to chirally quantify a ternary mixture of optical isomers [19], as well as a ternary mixture of three different amino acids [20]. In addition, isomeric (positional and isobaric) dipeptide [21] and tripeptide [22] mixtures have been quantified. In all these studies, chiral and isomeric distinction was achieved by investigating the dissociation kinetics of the transition metal-bound trimeric cluster ions. The main advantages of this approach are: (i) large chiral and isomeric differentiation; (ii) insensitivity to impurities since tandem mass spectrometry (MS/MS) is used; (iii) no requirement for isotopic labeling; (iv) independence of the result on the relative concentrations of the analyte and the reference ligand. It should be noted that a number of alternative mass spectrometric approaches to chiral analysis, often based on ion/molecule reactions, also exist and these should also be applicable to the distinction of mixtures of other types of isomers [23]. Tabet in particular has done important work on epimer distinction and chiral analysis by mass spectrometry [9].

Here we evaluate the capability of the kinetic method [7,8,24] for the differentiation and quantitation of isomers of peptides that include both  $\alpha$ ,  $\beta$ -amino acids by studying the dissociation kinetics of alkali metal and proton-bound dimers. The choice of dimeric rather than the trimeric clusters containing transition metal ions was in part made to facilitate determination of the structures of the cluster ions.

## 2. Experimental

All experiments were performed using a commercial LCQ ion trap mass spectrometer (Finnigan, San Jose, CA), equipped with an ESI source operated in the positive ion mode under the following conditions: spray voltage, 5.00 kV; capillary voltage, 20 V; heated capillary temperature, 150 °C; tube lens offset voltage, 20 V; sheath gas ( $N_2$ ) flow rate, 30 units (roughly 0.45 l/min). For the ion trap

mass analyzer, the automatic gain control (AGC) settings were  $5 \times 10^7$  counts for a full-scan mass spectrum and  $2 \times 10^7$  counts for a full product ion mass spectrum with a maximum ion injection time of 200 ms. In the full-scan MS/MS mode, the parent ion of interest was isolated by applying multiple waveforms to remove undesired ions through broadband excitation. The isolated ions were then subjected to a supplementary ac potential to resonantly excite them and so cause CID. The Mathieu  $q_z$  values chosen for resonance excitation and resonance ejection were 0.25 and 0.83, respectively. The excitation time used was 30 ms. Excitation amplitude can be varied from 0 to 100% relative collision energy corresponding to 0–2.5 V zero-to-peak resonant excitation potential; the value was optimized in each experiment, but kept constant for the measurement of the isomers. Spectra shown represent the average of  $\sim 50$  scans where each scan is an average of five individual microscans. Mass/charge ratios ( $m/z$ ) are reported using the Thomson unit (1 Th = 1 atomic mass per charge) [25].

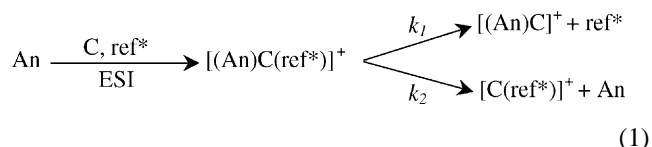
All amino acids in the tripeptides are named using the one-letter code. Gas-phase metal ion complexes with peptides were generated simply by electrospraying 50/50 water/methanol solutions containing a mixture of the analyte ( $\alpha$ - and/or  $\beta$ -amino acid containing tripeptide) and a reference tripeptide, at a concentration of 100  $\mu$ M each, together with 25  $\mu$ M of an alkali metal chloride. All tripeptides and alkali metal salts were purchased from Sigma Chemical Co. (St. Louis, MO) and used without further purification. Methanol (HPLC grade) was obtained from Fisher Co. (Pittsburgh, PA).

Optimized geometries and energies of idealized conformations were obtained by calculations with no symmetry constraints using Becke3LYP [26–28] DFT/HF hybrid functionals and 6-31+G(d,p) basis sets as implemented in Gaussian 98 [29].

## 3. Results and discussion

### 3.1. Methods for isomeric analysis by the kinetic method

The fundamental concept of isomeric mixture analysis of tripeptides containing  $\alpha$ ,  $\beta$ -amino acid is based on the kinetic method as illustrated in Eq. (1):



In this equation, C is the central ion (alkali metal ion or proton), An is the analyte tripeptide, and  $\text{ref}^*$  is a reference tripeptide.

The relative branching ratio  $R$  (Eq. (2)) for the two competitive dissociation channels is given by:

$$R = \frac{[(\text{An})\text{C}]^+}{[\text{C}(\text{ref}^*)]^+} \quad (2)$$

The relative branching ratios for the pure isomeric forms of the analytes (An), M and N, are  $R_M$  and  $R_N$ , while  $R_{iso}$  (a measure of isomeric selectivity) is given by the ratio of  $R_M$  and  $R_N$  (Eq. (3)):

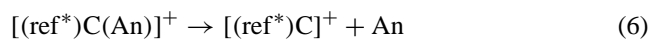
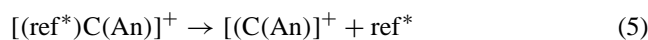
$$R_{iso} = \frac{R_M}{R_N} = \frac{[(An_M)C]^+ / [C(ref^*)]^+}{[(An_N)C]^+ / [C(ref^*)]^+} \quad (3)$$

The difference in energy required to generate the isomeric fragment ions  $[(An)C]^+$ , due to the two isomeric configurations of the analyte An, is reflected by the degree of isomeric distinction ( $R_{iso}$ ). The more difference the  $R_{iso}$  value from unity, the higher degree of isomeric recognition.

For a metal ion-bound cluster containing one reference ligand and one analyte ligand, the relationship between the relative branching ratio ( $R$ ) and the molar fraction of one isomer is given by the kinetic method [7,8] expression (Eq. (4)).

$$\ln R = \frac{\Delta(\Delta G)}{RT_{eff}} \quad (4)$$

Here  $R$  is the gas constant,  $T_{eff}$  is the effective temperature of the activated dimeric cluster ions (related to the average internal energy of the two activated complexes for the competitive dissociation channels [30]).  $\Delta(\Delta G)$  is defined as the difference in free energies for the reactions 5 and 6, whose reverse barriers are considered equal or negligible.



When the analyte consists of a pure isomer, viz.  $An_M$  and  $An_N$ ,  $\Delta(\Delta G)$  becomes  $\Delta(\Delta G)_M$  and  $\Delta(\Delta G)_N$ , and Eq. (4) takes the forms of Eqs. (7) and (8):

$$\ln R_M = \frac{\Delta(\Delta G)_M}{RT_{eff}} \quad (7)$$

$$\ln R_N = \frac{\Delta(\Delta G)_N}{RT_{eff}} \quad (8)$$

For a binary mixture with an isomeric molar fraction of M given by  $\alpha_M$ , one can write:

$$\begin{aligned} \Delta(\Delta G) &= \alpha_M \Delta(\Delta G)_M + (1 - \alpha_M) \Delta(\Delta G)_N \\ &= \Delta(\Delta G)_N + (\Delta(\Delta G)_M - \Delta(\Delta G)_N) \alpha_M \end{aligned} \quad (9)$$

Hence, the relationship between  $R$  and  $\alpha_M$  can be expressed by combining Eqs. (3), (4), (7), (8) and (9) to obtain Eq. (10):

$$\begin{aligned} \ln R &= \frac{\Delta(\Delta G)_N}{RT_{eff}} + \frac{\Delta(\Delta G)_M - \Delta(\Delta G)_N}{RT_{eff}} \alpha_M \\ &= \ln(R_N) + \ln(R_{iso}) \alpha_M \end{aligned} \quad (10)$$

Eq. (10) predicts a linear relationship between the isomeric composition  $\alpha_M$  and the natural logarithm of the branching ratio  $R$ . What this analysis does not provide is information on the *quality of this relationship* which is controlled by the extent to which the approximations in the kinetic method derivation are satisfied. It is also worth pointing out that

Eq. (10) gives physical meaning to the calibration curves: The slope is equal to the natural logarithm of the isomeric selectivity and the intercept is the natural logarithm of the branching ratio when the analyte is pure  $An_N$ .

### 3.2. Formation and dissociation of cluster ions for isomeric distinction

Abundant alkali metal cluster ions were observed for three pairs of the tripeptides containing  $\alpha, \beta$ -amino acids,  $(\alpha\text{-A})GG/(\beta\text{-A})GG$ ,  $G(\alpha\text{-A})G/G(\beta\text{-A})G$ , and  $GG(\alpha\text{-A})/GG(\beta\text{-A})$ , in the ESI mass spectra of mixtures of tripeptides and alkali metal salts (e.g., LiCl, NaCl, KCl, RbCl, CsCl). A typical ESI-MS spectrum of a mixture (NaCl and  $G(\beta\text{-A})G$ , and GGL) is illustrated in Fig. 1. The spectrum shows several ions, including relatively abundant protonated and sodiated clusters (monomers, dimers, and trimers), especially those involving the reference tripeptide GGL, which has the higher proton and alkali metal affinities. Sodium-adducts associated with deprotonated tripeptides of GGL such as  $[(GGL)_3 - H + 2Na]^+$  and  $[(GGL)_3 - 2H + 3Na]^+$  (at  $m/z$  758 and 780 Th, respectively) were also observed.

Fig. 2 shows the product ion (MS/MS) spectrum of a typical dimeric cluster ion,  $[(GGL)(An)+Na]^+$  ( $An = G(\alpha\text{-A})G$  and  $G(\beta\text{-A})G$ ) at  $m/z$  471 which was mass-selected and dissociated. Fragmentation occurs simply by competitive loss of one or the other intact neutral ligand to form a pair of cationized monomers. The measured branching ratio for these competitive dissociations strongly depends on the properties of alanine ( $\alpha$ - or  $\beta$ -amino acid) in the tripeptide. When the analyte, An, is  $G(\alpha\text{-A})G$ , the branching ratio is 0.331, whereas it is 15.8 for  $G(\beta\text{-A})G$ . The isomeric selectivity,  $R_{iso}$ , is therefore 47.7 for this case under these conditions. Although it is possible to investigate the dissociation kinetics of alkali metal-bound trimers to achieve isomeric distinction, we use the dimers here to simplify the dissociation kinetics as well as to facilitate the discussion of the structures of these cluster ions. For isomeric distinction of  $(\alpha\text{-A})GG$  and  $(\beta\text{-A})GG$ ,  $K^+$  was chosen as the center metal ion and GGG as the reference ligand. As illustrated in Fig. 3, a value of 11.6 for the isomeric selectivity was obtained under optimized experimental conditions in this case.

### 3.3. Differentiation of isomeric peptides by the kinetic method

Three pairs of isomeric tripeptides containing  $\alpha$  and  $\beta$ -amino acids,  $(\alpha\text{-A})GG/(\beta\text{-A})GG$ ,  $G(\alpha\text{-A})G/G(\beta\text{-A})G$ , and  $GG(\alpha\text{-A})/GG(\beta\text{-A})$ , were chosen as the analytes and the results for isomeric differentiation of these three mixtures are summarized in Tables 1–3, respectively. Isomeric distinction was investigated for each individual pair of isomers just indicated; other experiments could be done by combining the positional isomers in pairs. An observed trend is that increasing the size of the central metal ion from the proton to cesium, decreases the isomeric selectivity in experiments

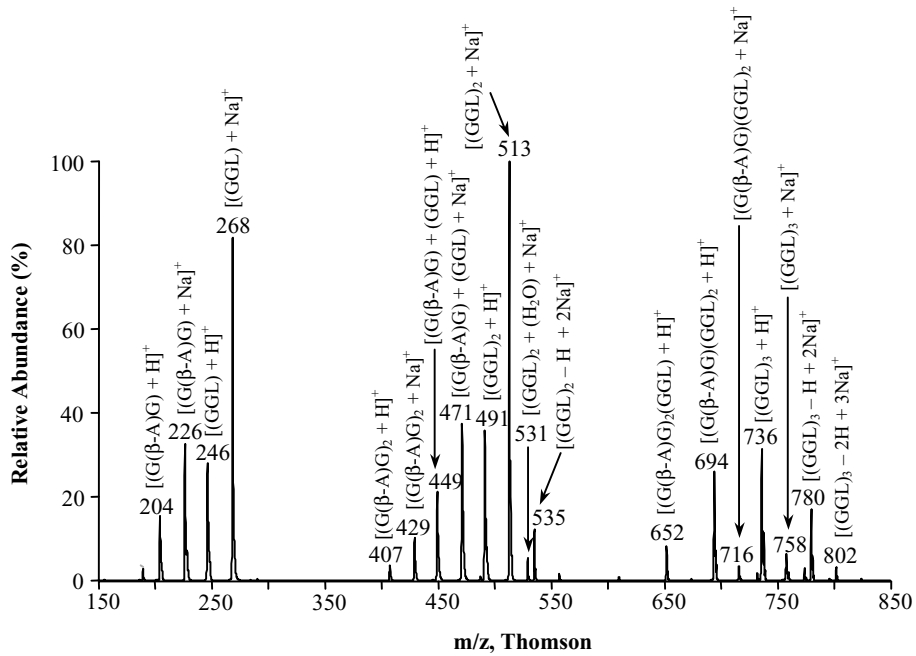


Fig. 1. ESI-MS spectrum of a mixture containing GGL, G( $\beta$ -A)G, and NaCl salt.

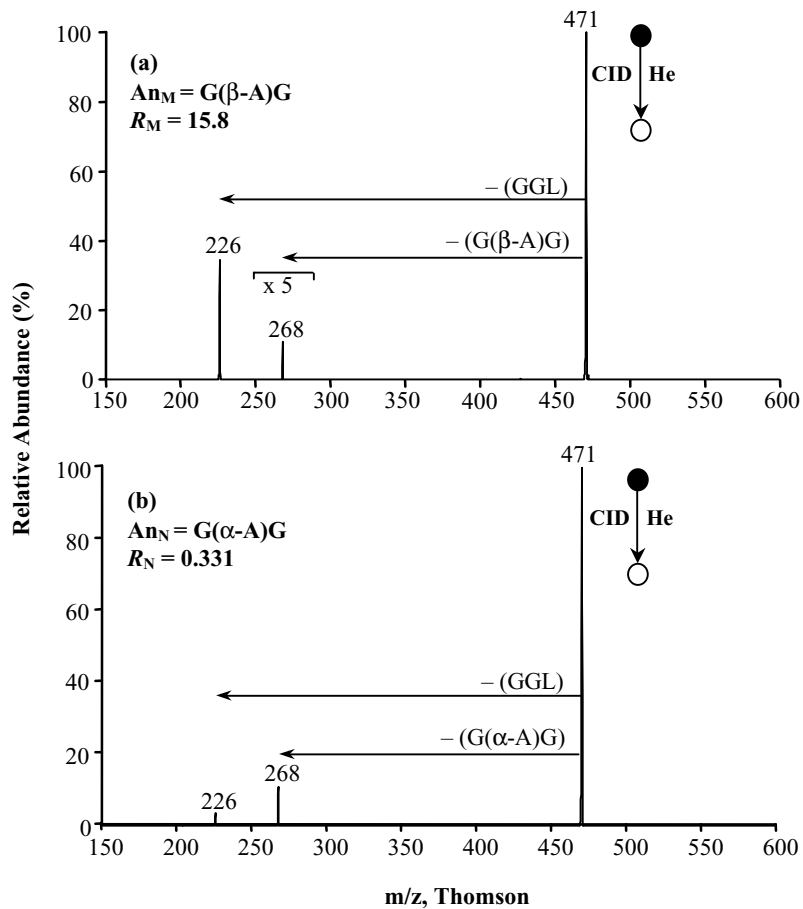


Fig. 2. MS/MS spectra of (a)  $[\text{GGL-Na-(G}(\beta\text{-A)G)]^+$  and (b)  $[\text{GGL-Na-(G}(\alpha\text{-A)G)]^+$ .

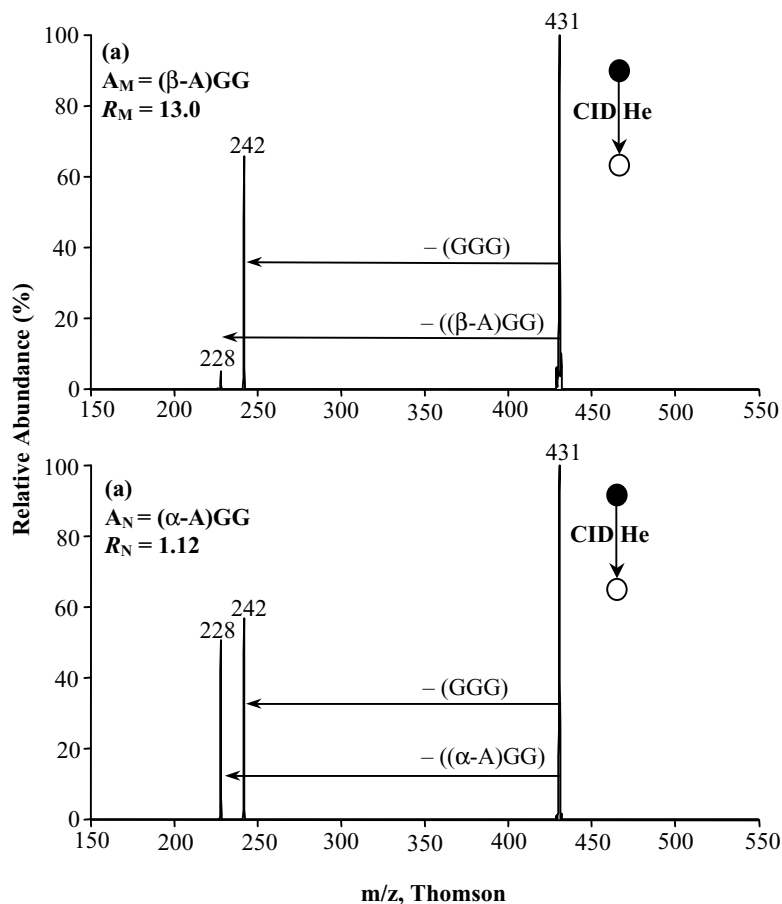


Fig. 3. MS/MS spectra of (a)  $[\text{GGG-K-(}\beta\text{-A)GG}]^+$  and (b)  $[\text{GGG-K-(}\alpha\text{-A)GG}]^+$ .

using three different tripeptides (GGL, GGI, and GGG) as references. The large isomeric selectivity for proton-bound clusters is speculated to result from entropy effects due to additional hydrogen-bonding. Among all the alkali metals, lithium gives the highest isomeric recognition most likely due to strong metal–ligand and ligand–ligand interactions.

Table 1  
Monovalent central ion and reference ligand effects on isomeric selectivity  $R_{\text{iso}}^{\text{a,b}}$

Central ion	$R_{\text{iso}}$		
	ref* = GGL	ref* = GGI	ref* = GGG
H <sup>+</sup>	2170 ± 701	2068 ± 585	2084 ± 662
Li <sup>+</sup>	2013 ± 140	1740 ± 310	1672 ± 312
Na <sup>+</sup>	188 ± 25	158 ± 12	214 ± 23
K <sup>+</sup>	34.1 ± 1.0	18.8 ± 0.5	11.6 ± 0.8
Rb <sup>+</sup>	15.0 ± 0.4	12.9 ± 0.4	8.41 ± 0.38
Cs <sup>+</sup>	11.5 ± 0.6	7.76 ± 0.24	6.64 ± 0.17

<sup>a</sup>  $(\alpha\text{-A)GG}/(\beta\text{-A)GG}$  ratios measured by dissociation of dimeric complexes, under identical conditions (isolation window 5 Th, relative CID collision energy of 10.5%, corresponding ca. 263 mV ac zero-to-peak excitation amplitude).

<sup>b</sup> The effective temperature  $T_{\text{eff}}$  is assumed as 850 K based on the study of the dissociation of proton-bound and alkali metal-bound clusters using He as collision gas.

All these trends are evident in the CID data for the proton- and alkali metal-bound cluster ions, as shown in Tables 1–3.

The peptides containing  $\beta$ -amino acids,  $(\beta\text{-A)GG}$ ,  $\text{G}(\beta\text{-A)G}$ , and  $\text{GG}(\beta\text{-A})$ , are non-chiral and changes in the reference ligands, such as from non-chiral peptides GGG to chiral peptides GGL and GGI, did not give a significant

Table 2  
Monovalent central ion and reference ligand effects on isomeric selectivity  $R_{\text{iso}}^{\text{a,b}}$

Central ion	$R_{\text{iso}}$		
	ref* = GGL	ref* = GGI	ref* = GGG
H <sup>+</sup>	202 ± 23	273 ± 41	235 ± 28
Li <sup>+</sup>	170 ± 13	198 ± 8	256 ± 8
Na <sup>+</sup>	22.5 ± 0.8	19.0 ± 1.1	18.4 ± 1.3
K <sup>+</sup>	16.6 ± 1.2	13.8 ± 1.5	13.3 ± 1.2
Rb <sup>+</sup>	8.86 ± 1.81	9.85 ± 1.92	8.86 ± 1.96
Cs <sup>+</sup>	6.31 ± 1.82	7.30 ± 1.62	5.88 ± 1.65

<sup>a</sup>  $\text{G}(\alpha\text{-A)G}/\text{G}(\beta\text{-A)G}$  ratios measured by dissociation of dimeric complexes, under identical conditions (isolation window 5 Th, relative CID collision energy of 10.5%, corresponding ca. 263 mV ac zero-to-peak excitation amplitude).

<sup>b</sup> The effective temperature  $T_{\text{eff}}$  is assumed as 850 K based on the study of the dissociation of proton-bound and alkali metal-bound clusters using He as collision gas.

Table 3  
Monovalent central ion and reference ligand effects on isomeric selectivity  
 $R_{\text{iso}}$ <sup>a,b</sup>

Central ion	$R_{\text{iso}}$		
	ref* = GGL	ref* = GGI	ref* = GGG
H <sup>+</sup>	18.7 ± 0.18	18.6 ± 0.18	19.8 ± 0.19
Li <sup>+</sup>	19.3 ± 0.20	19.5 ± 0.19	19.2 ± 0.19
Na <sup>+</sup>	9.83 ± 0.05	9.70 ± 0.09	9.05 ± 0.07
K <sup>+</sup>	3.38 ± 0.09	3.58 ± 0.06	3.29 ± 0.05
Rb <sup>+</sup>	2.91 ± 0.06	3.01 ± 0.08	2.89 ± 0.03
Cs <sup>+</sup>	2.57 ± 0.05	2.61 ± 0.03	2.66 ± 0.04

<sup>a</sup> GG( $\alpha$ -A)/GG( $\beta$ -A) ratios measured by dissociation of dimeric complexes, under identical conditions (isolation window 5 Th, relative CID collision energy of 10.5%, corresponding ca. 263 mV ac zero-to-peak excitation amplitude).

<sup>b</sup> The effective temperature  $T_{\text{eff}}$  is assumed as 850 K based on the study of the dissociation of proton-bound and alkali metal-bound clusters using He as collision gas.

increase in isomeric selectivity. This indicates that isomeric distinction in this case is an intrinsic result of changing the analyte tripeptides from  $\alpha$ -Ala to the  $\beta$ -Ala isomer. Note especially the sharp drop in isomeric selectivity observed when the position of the alanine changes from the N-terminus to the middle or to the C-terminus. Because the isomeric selectivity is directly related to the stability of the monomeric cluster ions that are associated with the two isomeric forms of the tripeptides, the large isomeric discrimination probably results from large differences in the structures of these cluster ions and hence in different metal-ligand interactions. This will be discussed in the following section.

### 3.4. Charge-solvated and zwitterionic (salt bridge) structures of cluster ions

The relative stabilities of the charge-solvated versus zwitterionic (salt-bridge) structures of amino acids and peptides in the gas phase have long been argued [31]. As metal cationized charge-solvated and zwitterionic forms can be interconverted by an intramolecular proton transfer process, the more stable zwitterionic structures are expected to be adopted by peptides when they are bound to large alkali metal ions such as Cs<sup>+</sup>, Rb<sup>+</sup>, and K<sup>+</sup>. In contrast, for the case of small alkali metals such as Li<sup>+</sup> and Na<sup>+</sup>, charge-solvated structures are more likely [32]. For the case of  $\beta$ -amino acid containing tripeptides bound to alkali metals, however, either structures might be favored; this is especially so in the tripeptide pair created by shifting alanine from the N-terminus to C-terminus. The nature (charge-solvated or zwitterionic) of the ion structure determines the stability of the cluster ions generated by either loss of the analyte or the reference, and hence determines the isomeric selectivity. Based on previous studies [32] on the structures of Li- and Na-bound clusters, Li- and Na-bound cluster ions are in general more stable in the charge-solvated than the zwitterionic form. In this study, the Li-bound peptides mainly fragment (as indicated using standard nomenclature [33]) to give  $[b_2 + H_2O + Li]^+$ , favoring the charge-solvated structure for both  $[GG(\alpha\text{-A}) + Li]^+$  and  $[GG(\beta\text{-A}) + Li]^+$ . This is consistent with the above conclusion that isomeric selectivity for differentiation of GG( $\alpha$ -A) and GG( $\beta$ -A) is relatively small. Note the  $b_n$  and  $y_n$  peptide fragments as illustrated in Scheme 1. By contrast, the fragment  $[b_2 + H_2O + Li]^+$  is the base peak when  $[GG(\beta\text{-A}) + Li]^+$  is the precursor ion, whereas the relative

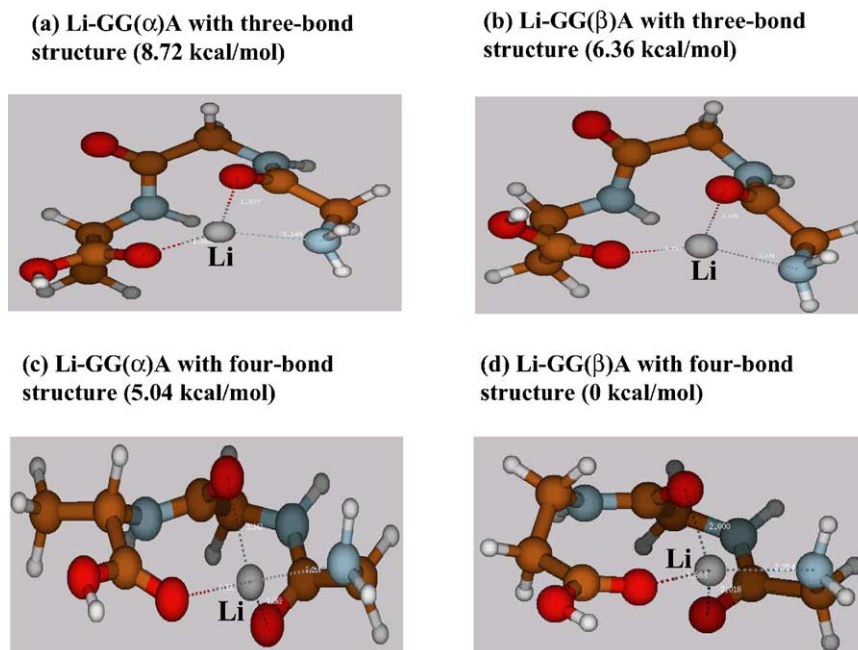
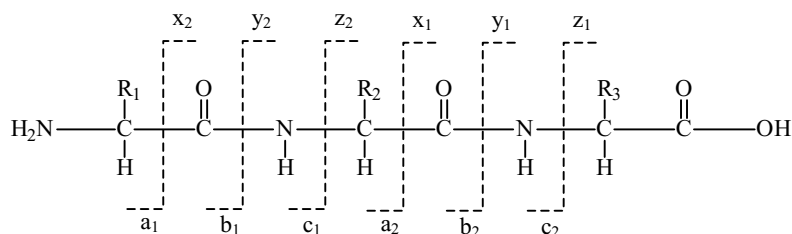


Fig. 4. Molecular calculation of Li-bound tripeptides using Becke3LYP DFT/HF hybrid function and 6-31+G(d,p) basis sets.





Scheme 1.

abundance of the same fragment is only 27% from dissociation of  $[GG(\alpha\text{-A}) + Li]^+$ .

High level molecular calculation employing Becke3LYP DFT/HF hybrid function and 6-31+G(d,p) basis sets (see Fig. 4) was used to obtain the optimized structures of the lithium-bound peptide. The results show four-bond structures are more likely compared to the three-bond struc-

tures for both  $[GG(\alpha\text{-A}) + Li]^+$  and  $[GG(\beta\text{-A}) + Li]^+$  (Fig. 4). Since  $\beta\text{-Ala}$  is one-carbon longer than  $\alpha\text{-Ala}$ , this makes  $GG(\beta\text{-A})$  more flexible when bonding to lithium and hence allows it to yield a more stable structure. In addition, avoidance of steric interactions associated with the methyl side chain in  $\alpha\text{-Ala}$  (no side chain in  $\beta\text{-Ala}$ ) weakens the oxygen of Ala interaction with Li. This is re-

Table 4  
Fragments of protonated and alkali metal-bound tripeptides

Parent ion	Fragments (relative abundance %)
<b>Lithiated</b>	
$[GG(\alpha\text{-A}) + Li]^+$	$[b_2 + H_2O + Li]^+$ (27%), $[M - (H_2O + NH_3) + Li]^+$ (12%), $[M - H_2O + Li]^+$ (25%)
$[GG(\beta\text{-A}) + Li]^+$	$[b_2 + H_2O + Li]^+$ (100%), $[b_1 + Li]^+$ (5%), $[M - H_2O + Li]^+$ (44%)
$[G(\alpha\text{-A})G + Li]^+$	$[y_1 + Li]^+$ (10%), $[b_2 - CO + Li]^+$ (7%), $[b_2 + Li]^+$ (31%), $[M - (H_2O + CO_2) + Li]^+$ (8%), $[b_2 + H_2O + Li]^+$ (24.2%), $[M - (H_2O + NH_3) + Li]^+$ (4%), $[M - H_2O + Li]^+$ (62%)
$[G(\beta\text{-A})G + Li]^+$	$[b_2 + Li]^+$ (15%), $[b_2 + H_2O + Li]^+$ (29%), $[M - H_2O + Li]^+$ (4%)
$[(\alpha\text{-A})GG + Li]^+$	$[y_1 + Li]^+$ (6%), $[b_2 + Li]^+$ (11%), $[y_2 + Li]^+$ (13%), $[b_2 + H_2O + Li]^+$ (11%), $[M - (H_2O + NH_3) + Li]^+$ (5%), $[M - H_2O + Li]^+$ (21%)
$[(\beta\text{-A})GG + Li]^+$	$[b_2 + Li]^+$ (18%), $[b_2 + H_2O + Li]^+$ (37%), $[b_2 + CO + Li]^+$ (8%), $[M - (H_2O + NH_3) + Li]^+$ (4%), $[M - H_2O + Li]^+$ (9%), $[M - NH_3 + Li]^+$ (4%)
<b>Sodiated</b>	
$[GG(\alpha\text{-A}) + Na]^+$	$[y_1 + Na]^+$ (19%), $[b_2 + Na]^+$ (3%), $[b_2 + H_2O + Na]^+$ (100%), $[M - H_2O + Na]^+$ (16%)
$[GG(\beta\text{-A}) + Na]^+$	$[y_1 + Na]^+$ (8%), $[b_2 + H_2O + Na]^+$ (22%), $[M - (H_2O + NH_3) + Na]^+$ (10%), $[M - H_2O + Na]^+$ (12%)
$[G(\alpha\text{-A})G + Na]^+$	$[y_1 + Na]^+$ (66%), $[b_2 + Na]^+$ (46%), $[b_2 + H_2O + Na]^+$ (7%), $[M - H_2O + Na]^+$ (97%)
$[G(\beta\text{-A})G + Na]^+$	$[y_1 + Na]^+$ (7%), $[b_2 + Na]^+$ (30%), $[b_2 + H_2O + Na]^+$ (12%), $[M - H_2O + Na]^+$ (9%)
$[(\alpha\text{-A})GG + Na]^+$	$[y_1 + Na]^+$ (30%), $[b_2 + Na]^+$ (28%), $[b_2 + H_2O + Na]^+$ (10%), $[M - H_2O + Na]^+$ (45%)
$[(\beta\text{-A})GG + Na]^+$	$[y_1 + Na]^+$ (25%), $[b_2 + Na]^+$ (13%), $[b_2 + H_2O + Na]^+$ (14%), $[b_2 + CO + Na]^+$ (42%), $[M - (H_2O + NH_3) + Na]^+$ (33%), $[M - H_2O + Na]^+$ (14%), $[M - NH_3 + Na]^+$ (6%)
<b>Potassium</b>	
$[GG(\alpha\text{-A}) + K]^+$	$[M - CO + K]^+$ (4%)
$[GG(\beta\text{-A}) + K]^+$	$[M - CO + K]^+$ (2%)
$[G(\alpha\text{-A})G + K]^+$	$[M - CO + K]^+$ (14%)
$[G(\beta\text{-A})G + K]^+$	$[M - CO + K]^+$ (10%)
$[(\alpha\text{-A})GG + K]^+$	$[M - CO + K]^+$ (89%)
$[(\beta\text{-A})GG + K]^+$	$[M - CO + K]^+$ (40%)
<b>Rubidium</b>	
$[GG(\alpha\text{-A}) + Rb]^+$	$Rb^+$ (100%)
$[GG(\beta\text{-A}) + Rb]^+$	$Rb^+$ (100%)
$[G(\alpha\text{-A})G + Rb]^+$	$Rb^+$ (100%)
$[G(\beta\text{-A})G + Rb]^+$	$Rb^+$ (100%)
$[(\alpha\text{-A})GG + Rb]^+$	$Rb^+$ (100%)
$[(\beta\text{-A})GG + Rb]^+$	$Rb^+$ (100%)
<b>Cesium</b>	
$[GG(\alpha\text{-A}) + Cs]^+$	$Cs^+$ (100%)
$[GG(\beta\text{-A}) + Cs]^+$	$Cs^+$ (100%)
$[G(\alpha\text{-A})G + Cs]^+$	$Cs^+$ (100%)
$[G(\beta\text{-A})G + Cs]^+$	$Cs^+$ (100%)
$[(\alpha\text{-A})GG + Cs]^+$	$Cs^+$ (100%)
$[(\beta\text{-A})GG + Cs]^+$	$Cs^+$ (100%)

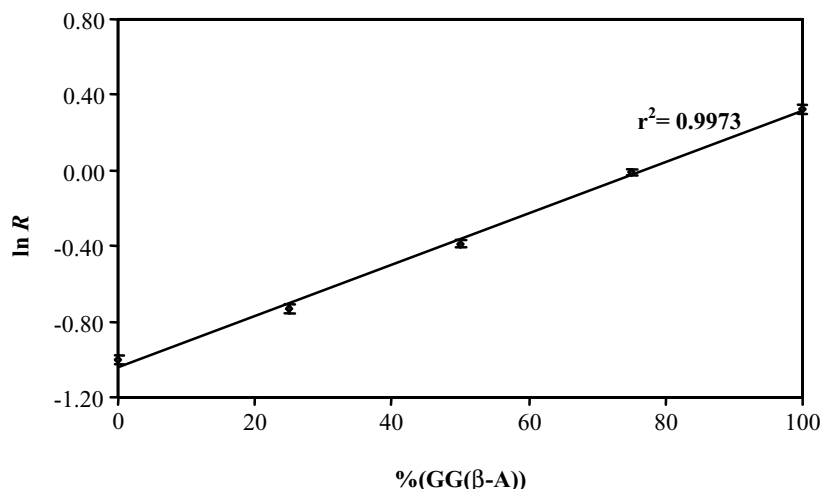


Fig. 5. Calibration curve for analysis of GG(β-A)/GG(α-A) using the Na<sup>+</sup> as the central metal ion and GGL as the reference ligand.

flected by the bond length of Li-O(Ala) which is shorter for β-Ala (1.883 Å) than α-Ala (1.931 Å). The overall energy for [GG(β-A) + Li]<sup>+</sup> is 5.04 kcal/mol lower than [GG(α-A) + Li]<sup>+</sup>. If one assumes an effective temperature for the activated cluster of 850 K, then this energy difference is consistent with the measured isomeric selectivity  $R_{iso}$ , a value of around 19. Further calculations were done and the results show that the peptides in the zwitterionic form are of higher energy than the charge-solvated structures. However, when alanine is shifted from the C-terminus to the middle, viz. in G(α-A)G and G(β-A)G, a new [y<sub>1</sub> + Li]<sup>+</sup> fragment arises from [G(α-A)G + Li]<sup>+</sup>, but not from [G(β-A)G + Li]<sup>+</sup>. When alanine is at the N-terminus, there is an additional [y<sub>2</sub> + Li]<sup>+</sup> fragment from [(α-A)GG + Li]<sup>+</sup>, but not from fragment [(β-A)GG + Li]<sup>+</sup>. This means that there are increasing contributions from zwitterionic structures in the cluster ions [G(α-A)G + Li]<sup>+</sup> and [(α-A)GG + Li]<sup>+</sup>, but not [G(β-A)G + Li]<sup>+</sup> and [(β-A)GG + Li]<sup>+</sup>. This causes the difference in stability of Li-bound peptides to increase and hence the isomeric selectivity becomes larger. Similar trends were also observed for Na-bound clusters (Table 4). For the case of K<sup>+</sup>, the loss of the intact tripeptides and CO<sub>2</sub> from the C-terminus indicates that the K-bound clusters are all in similar charge-solvated structures, reflected by the small isomeric selectivity for all three pairs of tripeptides. When Rb<sup>+</sup> and Cs<sup>+</sup> are chosen as the central metal ions, complete loss of the intact peptides for α- or β-amino acid containing tripeptides. The cluster ions appear to have similar loosely metal-bound charge-solvated structures and hence small difference in stability and isomeric selectivity. All these experimental results are supported by the theoretical calculations.

### 3.5. Quantitative analysis of isomeric peptides

The formation of the desired cluster ions is essential to successful isomeric analysis using the kinetic method. In this diagnostic study, we chose Na<sup>+</sup> and H<sup>+</sup> as the central

ions C, GGL as the reference ligand, and varied the concentration ratios of tripeptides GGA and GG<sub>V</sub>. The cluster ions [(GGA)C(GGL)]<sup>+</sup> and [(GGV)C(GGL)]<sup>+</sup> (C=Na<sup>+</sup> or H<sup>+</sup>) were readily generated by electrospraying a solution (comprised of NaCl, GGL, GGA or GG<sub>V</sub>). From the mass spectra, the measured intensity ratios of [(GGA)C(GGL)]<sup>+</sup> over [(GGV)C(GGL)]<sup>+</sup> was found to vary linearly with the concentration ratio of [GGA] over [GG<sub>V</sub>], e.g., a correlation coefficient of 0.9994 was recorded for Na<sup>+</sup> as the central ion and 0.9996 for H<sup>+</sup> as the central ion. This independence of experimental effects on cluster ion formation is an essential condition for isomeric mixture analysis.

Quantification was done using the reference and the analyte in various isomeric purities. Choosing Na<sup>+</sup> as the central metal ion, and GGL as the reference ligand, calibration curves for quantification of GG(β-A) in the mixture of GG(α-A)/GG(β-A) were constructed. The ratio  $R$  of the two fragment ions was measured in a single tandem (MS/MS) spectrum as a function of the isomeric purity of the analyte. As illustrated in Fig. 5, a linear relationship of ln  $R$  versus ee values (as predicted by Eq. (10)) was confirmed with a correlation coefficient ( $r^2$ ) of 0.9973. By using the calibration curves recorded under optimized experimental conditions, the isomeric peptides can be readily quantified. It is to be noted that when the isomeric selectivity is too large, i.e., larger than 20, the difference in the effective temperatures corresponding to the two individual dissociations associated with two forms of analytes will be significant. As a result, the calibration curve will take on curvature. This more complicated case is beyond the scope of this study and, in any event, very large ratios cannot be measured with high accuracy.

## 4. Conclusions

The kinetic method is used to differentiate and quantify mixtures of isomeric tripeptides based on the compet-



itive dissociations of alkali metal ion-bound dimeric clusters in an ion trap mass spectrometer. This methodology is efficient and allows recognition and quantification of three pairs of isomers:  $(\alpha\text{-A})\text{GG}/(\beta\text{-A})\text{GG}$ ,  $\text{G}(\alpha\text{-A})\text{G}/\text{G}(\beta\text{-A})\text{G}$ , and  $\text{GG}(\alpha\text{-A})/\text{GG}(\beta\text{-A})$ . The isomeric selectivity increases with decreasing size of the metal ions, viz. from Cs to Rb to K to Na to Li. It is also found that  $(\alpha\text{-A})\text{GG}/(\beta\text{-A})\text{GG}$  complexes show dramatically increased isomeric selectivity when alanine is at the N-terminus. When the proton is employed as the central ion, it gives similar behavior to Li. Differences in the structures of charge-solvation and zwitterion of the alkali metal-bound clusters, reflected by the  $b_n$  and  $y_n$  ions in tandem mass spectrometry, play a key role to promote isomeric differentiation. For small cations such as  $\text{Li}^+$  and  $\text{Na}^+$ ,  $(\alpha\text{-A})\text{GG}$  gives more zwitterionic structures while  $(\beta\text{-A})\text{GG}$  gives more charge-solvated structures, as supported by CID experiments. There is no discrimination in the formation of proton and alkali metal-bound dimers, and this forms the basis of isomeric quantification. While log/linear relationships are recorded, allowing the analytical methodology to be applied with confidence, the effects of activation conditions have not been investigated nor has the fundamental applicability of the kinetic method equation (Eq. (10)). This should be done in future as the kinetic method is explored as a possible way for future quantitative analysis of mixtures of larger peptides such as are generated, for example, in combinatorial synthesis of peptides and peptide mimics.

## Acknowledgements

This work is supported by US Department of Energy, Office of Basic Energy Sciences and by the National Science Foundation (Grant CHE 97-32670). Lianming Wu would like to thank the 2003 American Chemical Society-Division of Analytical Chemistry Graduate Fellowship Award sponsored by Johnson & Johnson Pharmaceutical Research and Development. E.M. and M.E. acknowledge FAPESP.

## References

- [1] J.L.G. Cole, M. Victor, *Biochemistry* 40 (19) (2001) 5633; J.L.G. Cole, M. Victor, *Biochemistry* 40 (2001) 5633.
- [2] S. Hanessian, X. Luo, R. Schaum, S. Michnick, *J. Am. Chem. Soc.* 120 (1998) 8569.
- [3] R.P. Cheng, S.H. Gellman, W.F. DeGrado, *Chem. Rev.* 101 (2001) 3219.
- [4] B.M. Olivera, D.R. Hillyard, M. Marsh, D. Yoshikami, *Trends Biotechnol.* 13 (1995) 422.
- [5] C.A.S. Barnes, A.E. Hilderbrand, S.J. Valentine, D.E. Clemmer, *Anal. Chem.* 74 (2001) 26.
- [6] M.R. Larsen, P. Roepstorff, *Fresen. Anal. Chem.* 366 (2000) 677.
- [7] R.G. Cooks, J.S. Patrick, T.S.A. McLuckey, *Mass Spectrom. Rev.* 13 (1994) 287.
- [8] R.G. Cooks, P.S.H. Wong, *Acc. Chem. Res.* 31 (1998) 379.
- [9] T.K. Majumdar, F. Clairet, J.C. Tabet, R.G. Cooks, *J. Am. Chem. Soc.* 114 (1992) 2897.
- [10] K. Vekey, G. Czira, *Anal. Chem.* 69 (1997) 1700.
- [11] J.B. Fenn, N. Mann, C.K. Meng, S.F. Wong, *Mass Spectrom. Rev.* 9 (1990) 37.
- [12] F. Hillenkamp, M. Karas, R.C. Beavis, B.T. Chait, *Anal. Chem.* 63 (1991) 1193A.
- [13] W.A. Tao, D. Zhang, F. Wang, P. Thomas, R.G. Cooks, *Anal. Chem.* 71 (1999) 4427.
- [14] L. Wu, W.A. Tao, R.G. Cooks, *Anal. Bioanal. Chem.* 373 (2002) 618.
- [15] W.A. Tao, R.G. Cooks, *Angew. Chem. Int. Ed.* 40 (2001) 757.
- [16] D.V. Augusti, F. Carazza, R. Augusti, W.A. Tao, R.G. Cooks, *Anal. Chem.* 74 (2002) 3458.
- [17] L. Wu, R.G. Cooks, *Anal. Chem.* 75 (2003) 678.
- [18] W.A. Tao, L. Wu, R.G. Cooks, *J. Med. Chem.* 44 (2001) 3541.
- [19] L. Wu, R.L. Clark, R.G. Cooks, *Chem. Commun.* 137 (2003) 136.
- [20] L. Wu, W.A. Tao, R.G. Cooks, *J. Mass Spectrom.* 38 (2003) 386.
- [21] W.A. Tao, L. Wu, R.G. Cooks, *J. Am. Soc. Mass Spectrom.* 12 (2001) 490.
- [22] L. Wu, K. Lemr, T. Aggerholm, R.G. Cooks, *J. Am. Soc. Mass Spectrom.* 14 (2003) 152.
- [23] J.C. Tabet, *Tetrahedron* 43 (1987) 3413.
- [24] R.G. Cooks, T.L. Kruger, *J. Am. Chem. Soc.* 99 (1977) 1279.
- [25] R.G. Cooks, A.L. Rockwood, *Rapid Commun. Mass Spectrom.* 5 (1991) 93.
- [26] A.D.J. Becke, *J. Chem. Phys.* 98 (1993) 5648.
- [27] C. Lee, W. Yang, R.G. Parr, *Phys. Rev. B* 37 (1988) 785.
- [28] P.J. Stephens, F.J. Devlin, C.F. Chabalowski, M.J. Frisch, *J. Phys. Chem. A* 98 (1994) 11623.
- [29] M.J. Frisch, G.W. Trucks, H.B. Schlegel, G.E. Scuseria, M.A. Robb, J.R. Cheeseman, V.G. Zakrzewski, J.J.A. Montgomery, R.E. Stratmann, J.C. Burant, S. Dapprich, J.M. Millam, A.D. Daniels, K.N. Kudin, M.C. Strain, O. Farkas, J. Tomasi, V. Barone, M. Cossi, R. Cammi, B. Mennucci, C. Pomelli, C. Adamo, S. Clifford, J. Ochterski, G.A. Petersson, P.Y. Ayala, Q. Cui, K. Morokuma, D.K. Malick, A.D. Rabuck, K.J.B. Raghavachari, J. Foresman, J.V. Cioslowski, B. Ortiz, B. Stefanov, G. Liu, A. Liashenko, P. Piskorz, I. Komaromi, R. Gomperts, R.L. Martin, D.J. Fox, T. Keith, M.A. Al-Laham, C.Y. Peng, A. Nanayakkara, C. Gonzalez, M. Challacombe, P.M.W. Gill, B. Johnson, W. Chen, M.W. Wong, J.L. Andres, C. Gonzalez, M. Head-Gordon, E.S. Replogle, J.A. Pople, *Gaussian 98, Revision A.6. Gaussian* (1998).
- [30] J. Laskin, J.H. Futrell, *J. Phys. Chem. A* 104 (2000) 8829.
- [31] W.D. Price, R.A. Jockusch, E.R. Williams, *J. Am. Chem. Soc.* 120 (1998) 3474.
- [32] R.A. Jockusch, W.D. Price, E.R. Williams, *J. Phys. Chem. A* 103 (1999) 9266.
- [33] P. Roepstorff, W.J. Richter, *J. Mass Spectrom. Ion Processes* 118/119 (1992) 789.